MEASUREMENT OF PLASMA DENSITY IN MODERN FUSION DEVICES BY DISPERSION INTERFEROMETER

A. L. Solomakhin[1, 2], P. A. Bagryansky[1, 2], W. Biel[3], H. Dreier[4], S. V. Ivanenko[1], A. D. Khilchenko[1], Yu. V. Kovalenko[1, 2], A. N. Kvashnin[1], H. T. Lambertz[3], A. A. Lizunov[1, 2], A. V. Lvovskiy[2], V. Ya. Savkin[1]

[1]*Budker Institute of Nuclear Physics, 630090, Novosibirsk, Russia*
[2]*Novosibirsk State University, 630090, Novosibirsk, Russia*
[3] *Forschungszentrum Jülich GmbH, Association EURATOM-FZ Jülich, Institut für Plasmaphysik, Trilateral Euregio Cluster, 52425 Jülich, Germany*
[4]*Max-Planck-Institut für Plasmaphysik, EURATOM Association, Wendelsteinstr. 1, D-17491 Greifswald, Germany*

We propose to use dispersion interferometer for measurement of plasma density and control of plasma position on present and future fusion devices. Distinguishing feature of this scheme is probing of plasma on two wavelengths. Short-wave radiation is formed by method of frequency fundamental radiation doubling. Probing first and second harmonics rays are combined spatially at the same time. It allows to create interferometer which is sensitive only to dispersion of studied medium and weakly sensitive to vibration of optical elements. Designs of the optical system dispersion interferometer and results of plasma density measurements on GDT mirror and TEXTOR tokamak are presented.

I. INTRODUCTION

Interferometry is reliable method to measure and control electron density and plasma column position in various plasma study applications. Different types of interferometers are used nowadays in most plasma magnetic confinement devices like tokamaks, RFPs or mirror systems. Besides delivery of physical measurement information, interferometers are also applied to provide machine control functions like feedback signals to manipulate of plasma density and position. Traditionally, interferometers with spatial separation of measurement channels are more common at fusion installations. However, these set-ups have several intrinsic disadvantages like sensitivity to vibrations and other sources of the measurement arm length instability. Additionally, the use of massive vibration isolation structures encompassing the plasma volume to reduce influence of vibration is not always possible in modern tokamaks. Among other solutions to overcome the above mentioned problem, some schemes are widespread:

- Interferometers using far-infrared radiation (118 μm, 337 μm) [1].
- Two-color interferometers [2].
- Polarimeter based on the Faraday effect or the Cotton-Mouton effect [3].

Another solution is a dispersion interferometer (DI), also "second harmonics interferometer" [4-7], utilizes the same principle as for a two-color interferometer, namely, separation of probing beams in frequency. The essential distinctive feature is that the second probing beam is generated by partial conversion of the first (or fundamental) wave into second harmonic in a frequency doubler nonlinear crystal. Both fundamental (FH) and second harmonic (SH) waves propagate through the same path by the nature of SH generation. In the ideal case, the dispersion interferometer is only sensitive to the phase shift gained by the two waves in a medium. For plasma dispersion equation, this phase shift can be expressed as

$$\Delta\varphi = \frac{3e^2}{8\pi\varepsilon_0 mc^2}\lambda < n_e l >,$$

here λ is the FH wavelength and $<n_e l>$ is the line integrated electron density.

Since no reference arm is necessary in a DI approach, one can make the diagnostic design relatively compact with all optical elements arranged on a single breadboard. This solution was implemented in the single-channel DI [8] for TEXTOR tokamak and GDT mirror.

II. DI ON GDT MIRROR

The interferometer based on DI principle is developed on Gas Dynamic Trap (GDT). The optical scheme is shown in Fig. 1. The radiation of laser 1 is focused by spherical mirror in the frequency doubler crystal 2, in which the radiation of the first harmonic is

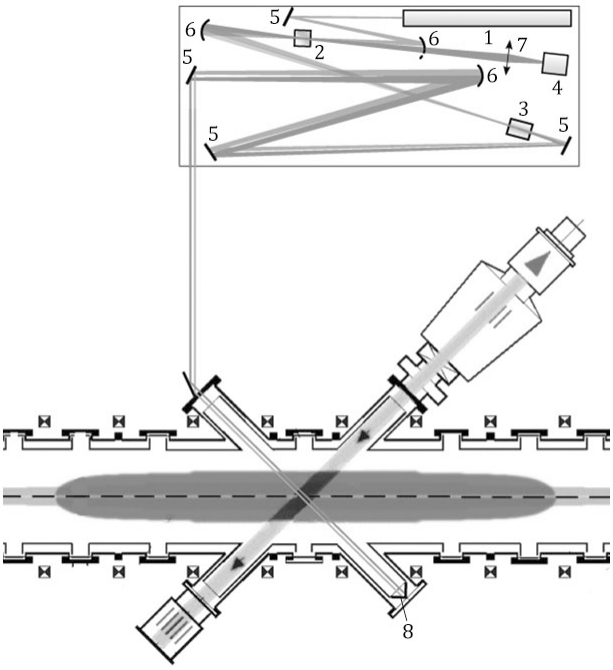

Fig. 1 Layout of the DI on GDT: 1 – CO_2 laser; 2 – frequency doubler; 3 – electro optical cell; 4 – photodetector; 5 – plane mirror; 6 – spherical mirror; 7 – lens; 8 – corner reflector.

partially converted to the second harmonic. Then the beam containing radiation at two wavelengths is focused in electro-optical cell (EOC) 3 which is used for modulation of wave phase. Then radiation is injected into vacuum chamber of a GDT through a plane–parallel BaF_2 window, where, after passing through plasma, it reflects from corner 8. The incident beam displaces relative to the centre of this reflector; consequently, the reflected beam does not coincide spatially with the incident beam but propagates in parallel through the optical system in the reverse direction. Thus the radiation crosses the plasma twice. After the second passage through the non-linear crystal, the first harmonic radiation is partially converted to the second harmonic for the second time. As a result, the beam contains three types of radiation: the first harmonic, the second harmonic produced after the first passage through the crystal, and the second harmonic produced after the second passage through the crystal. A mutual shift of the forward and backward beams allows to separate the backward beam from the forward beam on the one of mirrors. The backward beam is focused by lens 7 to photodetector 4, at whose entrance a sapphire (Al_2O_3) filter is fixed to absorb the first harmonic radiation. All of the optical elements are arranged on separate optical mount, except for the corner reflector attached to the wall of the vacuum chamber and two intermediate mirrors attached to lab wall and vacuum chamber.

The light source is cw CO_2-laser LCD-15WG with wavelength 9.57 μm and actual output power about 8 W. The non-linear crystal is $ZnGeP_2$ 5*5*5 mm. The electro-optical cell is GaAs 55*10*5 mm. We used photo detector PDI-2TE-5 from VIGO System S.A., with a double-stage Peltier cooling element. This detector has its maximum spectral sensitivity close to the second harmonic wavelength (5 μm).

We used technique of a phase modulation by EOC for increase measurable phase-shift range and decrease sensitive to variation amplitude of the signal. A sine voltage at a frequency of ~250 kHz and amplitude of ~3 kV was applied to the EOC. This corresponded to the half-wavelength voltage (the additional phase incursion is π). We developed special program algorithm, which using digitised signals from photo detector and electro-optical cell restore on a PC line-integrated electron density.

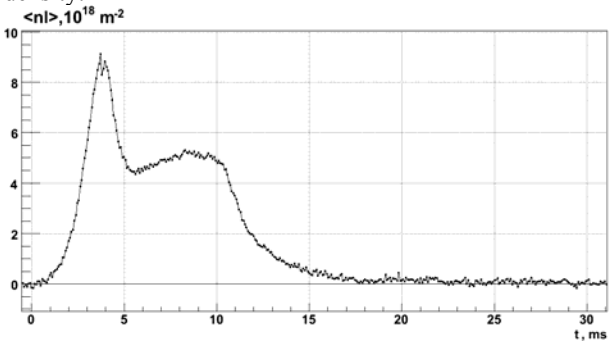

Fig. 2. Normal shot on GDT.

Dispersion interferometer measured line plasma density in the central section of GDT for demonstration of line density evolution. The typical result of line plasma density measurement in GDT is presented in Fig. 2. The minimal line plasma density measurable with the DI is $\langle n_e l \rangle \sim 10^{13}$ cm^{-2}, the time resolution is 100 μs.

III. DI ON TEXTOR TOKAMAK

DI concept was being developed on TEXTOR tokamak for number of years [4, 8]. This development work served as the basis for a multichannel dispersion interferometer using a CO_2 continuous wave laser. The primary aims and performance characteristic of the multichannel dispersion interferometer for TEXTOR are:

- 14 viewing lines (12 vertical and 2 diagonal);
- measurement of plasma density spatial profile;
- real-time control of the plasma density as well as the horizontal and vertical plasma positions;
- development and validation of techniques consistent with “next step” devices for fusion experiments such as Wendelstein 7-X and ITER.

III.A. DI Design

The projected multichannel dispersion interferometer has a modular design, which offers high flexibility in diagnostic deployment and configuration and also enables one to interchange different interferometer modules. The main challenge in the realization of a single module of DI (SIMDI) is the development of a compact and robust optical and mechanical design ensuring vibration compensation for the optical elements along the line of sight.

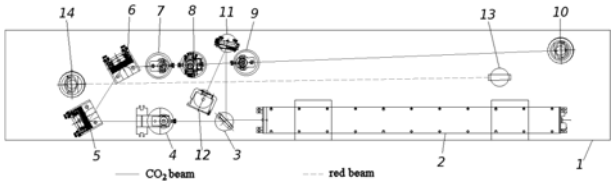

Fig. 3. Layout of the "laser level" of SIMDI: 1 – breadboard; 2 - CO_2 laser; 3, 11 – beam splitter plate; 4 – beam shutter; 5, 6 – plane mirror; 7, 9 – lens; 8 – aperture; 10, 14 – periscope mirror; 12 – power monitor; 13 – red laser.

Central element of the SIMDI is a horizontally mounted solid aluminium breadboard, elements of the SIMDI are arranged on both sides of this breadboard as shown in Figs. 3 and 4. The interferometer module is based on the cw 10.6 μm CO_2 laser SYNRAD J48-2W with output power 30 W 2. Beam splitters 3 and 11 in Fig. 3 reflect a small portion of the FH radiation to the laser power monitor 12 for a continuous control of the CO_2 source status. Two lenses 7 and 9 form a telescope with an aperture 8 in the beam waist: these elements provide a spatial separation of the probing and the backward beam to avoid undesirable additional interferometric effects. The periscope 10 reflects the probing beam by 90° to the other side of the breadboard 1, where receiver is periscope head 1 in Fig. 4.

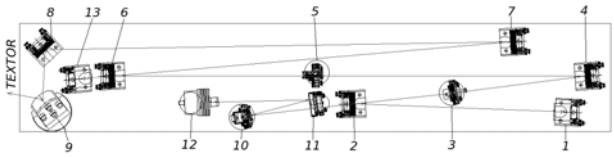

Fig. 4. Layout of the "optical level" of SIMDI: 1, 13 – periscope head; 2, 4, 7 – spherical mirror; 3 – frequency doubler; 5 – electro optical cell; 6, 8, 9, 11 – plane mirror; 10 – beam position monitor; 12 - photodetector.

Optical design of the SIMDI other side (Fig. 4) recalls optical design DI on GDT. The beam is focused in the frequency doubler crystal $AgGaSe_2$ 3. Then it is focused in the EOC 5 and is sent through the bottom flange in the vacuum vessel, passes through the plasma and reflects from the corner reflector which is placed on the other side. The reflected backward beam is slightly vertically shifted. This allows to separate the backward beam from the original one at the mirror 2, where the upper half of the mirror is cut off. After separation at half-mirror 2, the backward beam is focused to the main photodetector 12. The photodetector uses a sapphire filter, which is transparent for the 5.3 μm wavelength but it absorbs the remaining 10.6 μm beam fraction. Thus the interference signal produced by two SH waves is analysed. In addition, the mirror 10 contains four small (1.5*1.5 mm) thermopile sensors arranged in a rectangular pattern. These sensors measure the position of the backward beam and are used for continuous monitoring of the status of in-vessel beam formation optics. Numerical simulations have been used to precalculate the optimal beam characteristics, the focal lengths of spherical mirrors 2, 4, and 7 have been chosen according to these calculations.

Element 5 is an EOC based on a GaAs crystal; application of voltage $U=U_o\sin(\omega t)$, (where U_0~4 kV, ω=250 kHz) leads to the beam phase sweep $-\pi...\pi$. The measurement technique based on the phase modulation (close to the well known zebra stripes method) is described in Ref. 6. The periscope head 13 in Fig. 4 receives the visible red beam (λ~0.6 μm), the plane mirror 6 is equipped with a small hole in the center to align the red beam with the CO_2 beam.

Multichannel design of the DI on TEXTOR allows to install 12 SIMDI modules actually. We created and installed 4 SIMDI modules (Tabl. 1):

TABLE I. Mounted channel

Channel number	Distance from plasma center, mm
3	34
5	176
9	116
10	16

All 4 modules allow to measure the line-integrated plasma density along direct vertical chords and do not use in-vessel optics. Corner reflectors are installed on the top flange outside the vacuum chamber.

The control and data processing system of the 14-channel DI consists of two independent but interacting segments. All "standard" control functions and the monitoring of the SIMDI status signals are realized on the base of an industrial SIEMENS S7-300 controller at each module. This solution is consistent with modular structure of the diagnostic and permits easy integration into existing TEXTOR control system framework. The subsystem responsible for data acquisition is developed specially for the multichannel DI. Each SIMDI hosts the data processing electronic module based on a programmable logic matrix (PLM) core. The usage of a PLM for signal processing enables a guaranteed real-time rate of output $\langle n_e l \rangle$ values calculation, this approach also

gives flexibility to change programmed calculation algorithms. The real-time data processing module delivers output signal via the serial fiber line to the remote signal conditioning rack connected to TEXTOR engineering systems controlling [9].

III.B. DI Results

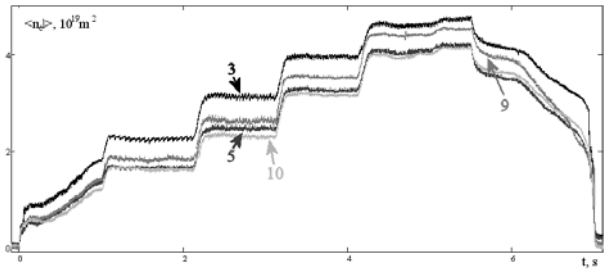

Fig. 5. Normal TEXTOR shot No. 113119.

Four channel DI has been tested in TEXTOR experiment. Fig. 5 shows line-integrated density plot obtained by this diagnostic in normal TEXTOR shot No. 113119. Fig. 6 shows achievable density resolution in shot No. 112787. Here is shown sawteeth oscillations, which measured by central (3, 10) DI channels.

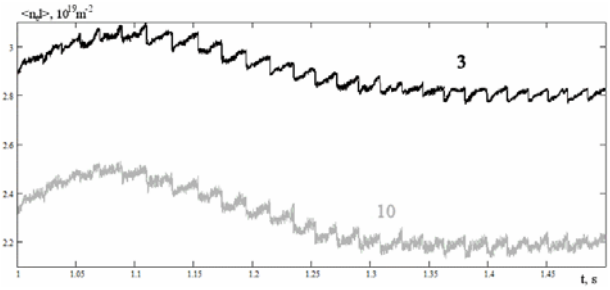

Fig. 6. Sawteeth oscillations of plasma in the shot No 112787.

We tested DI (Fig. 7) on special TEXTOR regime with big plasma disruption. DI demonstrated capability measuring on the regime with very big density and very big velocity of plasma density change.

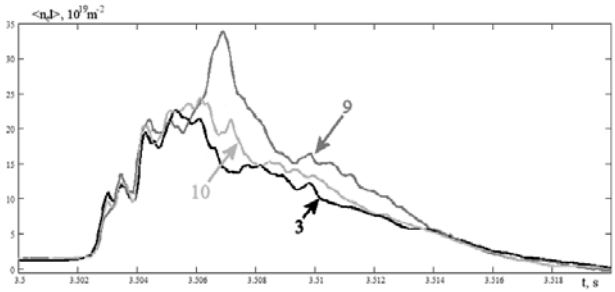

Fig. 7. Disruption in the shot No 112814.

IV. CONCLUSIONS

DI has been developed and tested on GDT mirror and TEXTOR tokamak. DI has shown the ability of measurement line-integrated electron density in modern fusion devices. DI will be used for measurement and control of plasma density and plasma position in modern and future fusion devices like ITER and W7-X.

ACKNOWLEDGMENTS

This work was supported by the Federal Education Agency (Contract No. P1580, P969), Analytical Department Target Program "The Development of Higher School Scientific Potential" (Project No. 2.1.1/579) and RF President's grant MD-2995.2009.2.

REFERENCES

1. H. R. KOSLOWSKI and H. SOLTWISCH, Fusion Eng. Des. 34, 143, (1997).
2. T. KONDOH, A. E. COSTLEY, T. SUGIE, Y. KAWANO, A. MALAQUIAS, and C. I. WALKER, Rev. Sci. Instrum. 75, 3420 (2004).
3. Y. KAWANO, S. CHIBA and A. INOUE, Rev. Sci. Instrum. 72, 1068 (2001).
4. P. A. BAGRYANSKY, A. D. KHILCHENKO, A. N. KVASHNIN, A. A. LIZUNOV, R. V. VOSKOBOYNIKOV, A. L. SOLOMAKHIN, and H. R. KOSLOWSKI (TEXTOR team), Rev. Sci. Instrum. 77, 053501 (2006).
5. F. A. HOPF, A. TOMITA and G. Al-JUMAILY, Optics letters 5, 386 (1980).
6. Kh. P. ALUM, Yu. V. KOVAL'CHUK and G. V. OSTROVSKAYA, Sov. Tech. Phys. Lett. 7, 581 (1981).
7. T. AKIYAMA, K. KAWAHATA, S. OKAJIMA and K. NAKAYAMA, Plasma Fusion Res. 5, S1041 (2010).
8. A. LIZUNOV, P. BAGRYANSKY, A. KHILCHENKO, Yu. V. KOVALENKO, A. SOLOMAKHIN, W. BIEL, H. T. LAMBERTZ, Yu. KRASIKOV, M. MITRI, B. SCHWEER and H. DREIER, Rev. Sci. Instrum. 79, 10E708 (2008).
9. A. D. KHIL'CHENKO, A. N. KVASHNIN, S. V. IVANENKO, P. V. ZUBAREV, D. V. MOISEEV and Yu. V. KOVALENKO, Instruments and Experimental Techniques 52 (3), 382-393 (2009).